Osteoarthritis and Cartilage Open 7 (2025) 100583

Contents lists available at ScienceDirect

Osteoarthritis and Cartilage Open

journal homepage: www.elsevier.com/journals/osteoarthritis-and-cartilage-open/2665-9131

Patients with unilateral patellofemoral pain have altered bone turnover in the painful knee compared to the pain-free knee at rest and after acute knee loading

Rudi Hansen [a,b,*], Bryan Haddock [c], René B. Svensson [b], Markus Nowak Lonsdale [d], Lisbeth Marner [d], Lene Rørdam [d], Inge Lise Rasmussen [d], Christoffer Brushøj [b], S. Peter Magnusson [a,b], Marius Henriksen [e], Christian Couppé [a,b]

[a] Department of Physical and Occupational Therapy, Copenhagen University Hospital Bispebjerg Frederiksberg, Copenhagen, Denmark
[b] Institute of Sports Medicine Copenhagen, Department of Orthopedic Surgery, Copenhagen University Hospital Bispebjerg Frederiksberg, Copenhagen, Denmark
[c] Department of Clinical Physiology, Nuclear Medicine and PET, Rigshospitalet, Copenhagen University Hospital, Denmark
[d] Department of Clinical Physiology & Nuclear Medicine, Copenhagen University Hospital Bispebjerg Frederiksberg, Copenhagen, Denmark
[e] The Parker Institute, Copenhagen University Hospital Bispebjerg Frederiksberg, Copenhagen, Denmark

ARTICLE INFO

Handling Editor: Professor H Madry

Keywords:
Patellofemoral pain
PFP
Bone turnover
Bone perfusion
Bone metabolism
Positron Emission Tomography
Na[^{18}F]F

ABSTRACT

Objective: The objective of this study was to investigate subchondral bone turnover at rest and after acute loading using Fluorine-18-labeled sodium fluoride (Na[^{18}F]F) Positron Emission Tomography (PET), in patients with unilateral PFP.

Design: Twenty-seven patients with unilateral PFP were recruited from the Institute of Sports Medicine Copenhagen. Participants underwent Na[^{18}F]F-PET imaging before and after a bout of single-leg squats. Bone turnover measures, including mean and maximal standardized uptake value (SUV_{mean} and SUV_{max}), rate of bone perfusion (K1), rate of tracer uptake into bone (Ki), and extraction fraction of tracer absorbed into bone mineral were assessed for patella and trochlea.

Results: At rest, the painful knees showed lower SUV_{max}, K_1, and K_i compared to the pain-free knees in the superficial part of the patella. No significant differences were found in the profound part of the patella or trochlea at rest. Following knee loading, the acute increases in SUV_{mean}, SUV_{max}, K_i and blood flow were reduced in the superficial patella of the painful knees compared to the pain-free knees. In the trochlea, painful knees showed larger increases in SUV_{mean} and K_i in the lateral part, whereas the medial part showed greater increases in K_1, K_i, and a larger decrease in extraction fraction after loading.

Conclusion: Patella displayed decreased bone metabolism at rest and reduced response to loading in the painful versus pain-free knees. Trochlea in the painful knees showed significantly larger increases in subchondral bone metabolism following knee loading compared to the pain-free knees. These novel findings highlight potential differences in bone turnover between the patellar and trochlear regions.

1. Introduction

Anterior knee pain (patellofemoral pain, PFP) is a common knee disorder that particularly affects young sports-active people [1]. The disorder is characterized by pain around the patella leading to physical inactivity, less participation in exercise and sports, and ultimately, reduced quality of life [1–3]. The prevalence in adolescents is 7 %, constituting 11–17 % of all knee problems seen by general practitioners, which makes it the most frequent nontraumatic diagnosis [4,5]. Recent research indicates that even after a 2-year follow-up, 65 % of adolescents

* Corresponding author. Department of Physical and Occupational Therapy, Copenhagen University Hospital Bispebjerg Frederiksberg, Nielsine Nielsensvej 10, DK-2400 Copenhagen, Denmark.

E-mail addresses: rudi.hansen@regionh.dk (R. Hansen), bryan.haddock@regionh.dk (B. Haddock), svensson.nano@gmail.com (R.B. Svensson), markus.nowak.lonsdale@regionh.dk (M. Nowak Lonsdale), lisbeth.marner@regionh.dk (L. Marner), lene.roerdam@gmail.com (L. Rørdam), inge.lise.rasmussen@regionh.dk (I.L. Rasmussen), chbr@teamdanmark.dk (C. Brushøj), p.magnusson@sund.ku.dk (S.P. Magnusson), marius.henriksen@regionh.dk (M. Henriksen), christian.couppe@regionh.dk (C. Couppé).

https://doi.org/10.1016/j.ocarto.2025.100583
Received 7 November 2024; Accepted 10 February 2025

diagnosed with PFP continue to experience knee pain, with 25 % reporting daily knee discomfort [1].

The reason for the development of PFP is still uncertain [6]. Patients with PFP have no observable structural damage to the soft tissues, bones, or cartilage in the joint assessed by conventional imaging [7]. The treatment of the disorder therefore often becomes non-specific, with considerable variation in treatment strategies among therapists [8]. A correlation has been found between PFP and the development of patellofemoral osteoarthritis (OA) later in life [9,10], and studies indicate that the pain may originate from the subchondral bone areas in the patellofemoral joint [11]. Subchondral bone is metabolically active, and changes in subchondral bone remodeling and vascularization have been implicated in early OA [12–14]. Experimental OA induction in animals supports the notion that subchondral bone changes may precede cartilage deterioration, suggesting a sequential relationship during OA development [13,15,16]. Notably, research in rabbit and mouse models has identified that articular cartilage degradation predominantly occurs in areas beneath thickened subchondral bone, whereas regions overlying normal bone remain unaffected [15,17]. These findings underscore the critical role of subchondral bone remodeling in the early stages of OA.

Positron Emission Tomography (PET) imaging of Fluorine-18-labeled sodium fluoride (Na[^{18}F]F) uptake has been used to detect altered bone metabolism, as it highlights areas of newly mineralizing bone and correlates well with bone histomorphometry [18,19]. Na[^{18}F]F PET has also been able to detect an acute hemodynamic response in bone immediately after loading with increased blood flow and total tracer uptake [20]. In patients with PFP, Na[^{18}F]F PET has shown increased bone remodeling in the subchondral bone structures of the knee joint [21], indicating a healing process and/or bone remodeling similar to that seen in early osteoarthritis [22,23]. In addition, an association could be demonstrated between increased bone activity and the magnitude of patients' knee pain and the location of the pain [21]. However, the study was performed on a very limited number of patients, and it therefore remains unknown if PFP is related to altered bone metabolism at rest and whether it affects the response to acute knee loading.

In this study, we aimed to include a larger population of patients with PFP using the same PET tracer (Na[^{18}F]F) to investigate, in a within-participant design, whether patients with unilateral PFP have increased bone turnover in the painful knees compared to the pain-free knees. In addition, the study investigated how acute loading affects bone perfusion and tracer extraction.

2. Methods

2.1. Population

This study is a sub-study of a larger randomized controlled trial and was approved by the Health Research Ethics Committee of Capital Region Denmark, number: H-16045755 (additional protocol number 64139, approved August 14, 2018). In the main study, participants were randomized to a 12-weeks intervention comprising exercises for either the quadriceps or for the hip muscles [24]. This present study was performed after inclusion but before initiation of the interventions. The participants were recruited from the Department of Sports Medicine Copenhagen (ISMC), Bispebjerg-Frederiksberg Hospital, Denmark. All potential participants were assessed by a sports medicine physician and included according to the following inclusion criteria: 1) A clinical diagnosis of PFP in only one knee; 2) A score of at least 3 on a 10 cm Visual Analogue Scale (VAS) pain scale during daily activities in the previous week; 3) Gradual onset of symptoms unrelated to trauma and lasting for at least 4 weeks; and 4) Pain associated with at least 3 of the following: During or after knee-loading activity, prolonged sitting with knees flexed, stair ascent or descent, squatting. Exclusion criteria included pregnancy, breast-feeding, contralateral knee pain during the previous 6 months, intra-articular knee injury and/or another overuse or traumatic knee injury. Prior to participating in the study, all subjects were informed about the study and provided written informed consent.

Fig. 1. Illustration of the setup for the knee loading regime. Participants performed the one-legged squat on a decline board with the upper body in an upright position and the arms crossed in front of the chest. The assessor closely monitored the exercise, providing feedback on the quality, cadence, and range of motion. A goniometer set at 60° was positioned near the participant's knee during the movement. If the participant failed to reach (or exceeded) the target flexion, they were encouraged to make the necessary adjustments.

2.2. PET/CT

Dynamic PET/Computed Tomography (CT) scans covering both knees were performed twice: before and after exercise using a GE Discovery 4-ring MI PET/CT system (axial Field of View (FOV) = 20 cm, GE Healthcare, Milwaukee, WI). To minimize the effects of recent physical activity and blood flow on tracer uptake, participants were instructed to abstain from engaging in strenuous physical activities such as cycling, extended walks, stair climbing, working on ladders, squatting, etc., for a period of 24 h preceding the examination. Furthermore, they were instructed to refrain from undertaking intense knee-loading exercises such as jumping, running, and cutting activities (i.e., sudden changes in direction while running or moving) for at least 48 h prior to the PET scans. On the day of the trial, the participants were not allowed to cycle, run, or walk (more than 500 m), when transporting themselves to the hospital.

Subjects were scanned in a supine position and the knees were flexed to approximately 30°, with a contoured pillow positioned beneath the knees. The legs were strapped together with an elastic wrap (Nylatex wrap, Chatanooga, DJO global, Dallas, Texas, USA) to minimize movement between the CT and PET scans. Each session started with a CT of both knees (120 kVp, dose modulated 49 mA). The acquired data were reconstructed into three datasets: A dataset exclusively used for PET attenuation correction, a second dataset for anatomical localization (slice thickness: 3.75 mm, matrix size: 512 × 512 pixels (0.98 mm)) and a third

Fig. 2. Segmentation using CT images: superficial patella (blue), profound patella (red), trochlea (green), central femur condyle (purple), posterior femur condyle (orange), and tibia plateau (yellow). (For interpretation of the references to color in this figure legend, the reader is referred to the Web version of this article).

dataset with a bone enhancement kernel using 50 % iterative reconstruction (slice thickness: 0.625 mm, matrix size: 512 × 512 pixels (0.98 mm)).

After the CT, a 1-h long, single-bed, list-mode PET acquisition was started and 90 MBq Na[^{18}F]F were injected. PET data were reconstructed in 67 frames (20 × 1 s, 10 × 10 s, 10 × 30 s, 5 × 60 s, 22 × 120 s, starting with the arrival of administered activity in the PET field-of-view). All PET reconstructions used CT for attenuation correction and a block-sequential regularized expectation-maximization penalized-likelihood reconstruction method (Q.Clear), including time-of-flight and point-spread-function information with relaxation parameter beta = 350. Matrix size was 192 by 192 pixels (2.73 mm) with a slice thickness of 2.79 mm.

2.3. Knee loading exercises

After the first PET scan, the participant performed 3 sets of 10 repetitions of one-legged squats (0–60° of flexion) on each leg while standing on a decline board with 25-degree slope [25]. The squats were performed one set at a time alternating between the painful and the pain-free leg. The starting leg was randomly assigned so that half of the participants started with the painful leg and the other half started with the pain-free leg. The participant was instructed to perform the squats with the upper body in an upright position and arms crossed at the chest at pace 2 s down and 2 s up (Fig. 1). A metronome was set at 30 beats per minute to keep pace. The participant was allowed to lightly touch the nearby wall for balance. There was a 1-min break between each set. The assessor monitored and gave feedback on the quality, cadence, and range of motion (knee flexion angle measured with a goniometer fixed at 60°) during the exercises to ensure a standardized performance.

2.4. Segmentation and preparation of data

Using the CT images, masks covering the femur, patella, and tibia were first created by manually drawing regions of interest (ROIs). The bone tissue was then segmented further to create subchondral/cortical bone masks using k-means clustering (4 cluster groups minimized to squared Euclidean distance repeated 4 times with different initial centroids). The long bones of the femur and tibia were manually identified as the cortical bone 6–8 cm from the center of the joint space. The subchondral and cortical bone of the femur and patella was manually subdivided into regions: medial and lateral part of trochlea, superficial and profound part of patella, central and posterior regions of the medial and lateral femoral condyle (Fig. 2). Lastly, cortical bone at the site of the patellar tendon insertion (tibial tuberosity) was identified and excluded from the analysis of cortical bone.

Image co-registration, ROI analysis, and calculations of uptake values and kinetic parameters were performed with custom software created in MATLAB 2016b (MathWorks, Natick, MA, USA). Segmentation into anatomical regions and bone type (cortical, trabecular) was done semi-automatically using CT-images. Segmentation was based on bony landmarks unrelated to PET-data and blinding was therefore not relevant.

2.5. SUV and kinetic uptake parameters

All SUV and kinetic parameter estimation was performed for individual subregions (Fig. 2). A single "static" frame covering the last 5 min was reconstructed for calculation of standardized uptake values (SUV). For the post-exercise PET acquisition, an initial 3-min frame for measuring and subtracting residual [^{18}F] concentration from the pre-exercise injection was performed. Then, the same protocol was followed for the baseline acquisition. In addition to measuring changes in SUV, kinetic modeling of dynamic Na[^{18}F]F uptake was performed to quantify different aspects of bone metabolism including rate of tracer uptake into bone (K_i), rate of bone perfusion (K_1), rate of tissue clearance (k_2), rate of bone mineralization (k_3), and the extraction fraction of tracer that is extracted to bone mineral. An image derived arterial input function (IDIF) was calculated based on the Na[^{18}F]F activity (kBq/mL) in the popliteal artery for each knee independently, following previously established methods [26]. We fitted the IDIF and tissue Time-Activity Curve (TAC) data to a Hawkins two-tissue tracer kinetic model using nonlinear regression (NLR), as detailed in other publications [20,26,27]. This fitting aimed to estimate the following rate constants: K_1 for bone perfusion (mL min^{-1} mL^{-1}), k_2 for tissue clearance (min^{-1}), and k_3 for mineralization (min^{-1}). The rate constant k_4, representing bone clearance, was assumed to be 0. NLR fitting to estimate these three rate parameters, along with parameters to account for partial volume fraction, blood fraction, and input dispersion estimate was performed for each bone subregion using COMKAT software [28].

We calculated the extraction fraction using the formula:

$$\text{Extraction fraction} = \frac{k_3}{k_2 + k_3}$$

which represents the proportion of ^{18}F entering the bone tissue that binds to the bone matrix, in contrast to being cleared back into the plasma pool and ranges in value from 0 to 1. The parameter K_i^{NLR} (K_i), the rate of clearance of ^{18}F from the plasma to the bone mineral compartment, was calculated using the formula [28]:

$$K_i = K_1 * \text{extraction fraction}$$

and has units of mL min^{-1} mL^{-1}.

2.6. Statistical analysis

The sample size was pragmatically based on an expected inclusion rate of 1:5 in the remaining 150 participants expected to be included in the main RCT at the starting date of this study, i.e., 30 participants. The proposed inclusion rate reflected the reported proportion of patients with unilateral symptoms vs. patients with bilateral symptoms, i.e., one in two to four (6, 7) adjusted for an anticipated rejection.

Statistical comparisons of measures between painful and pain-free knees at baseline, and the differences in delta values (the change between baseline and post-exercise) between painful and pain-free knees, were performed using a mixed-effects model. This model included knee

Table 1
Patient characteristics.

No. of patients (men/women)	27 (10/17)
Age (years)	26.1 ± 4.7
Weight (kg)	72.7 ± 13.5
Height (cm)	173.0 ± 10.9
BMI	24.2 ± 3.6
Duration of symptoms (months) (median (IQR))	24.0 (48)

The data are presented as means ± SD unless otherwise stated.
IQR: Interquartile range.

condition (painful vs. pain-free) as fixed effect and subject as random effect (random intercept). To reduce variance caused by differences in uptake in uninvolved tissues and better distinguish the involved tissues, analyses on normalized data were also performed. We normalized the data by dividing the raw values of the specific region by the values of the cortical bone of the ipsilateral tibia. Tibia was checked visually for focal increases in tracer uptake based on the static frame covering the last 5 min of the PET scan and was considered representative of background tracer uptake. Hence, a normalized value of 1 equals identical uptake values in the region of interest and the background uptake.

The residuals for both raw and normalized values met model assumptions of linearity and variance and were normally distributed. The mean and 95 % confidence intervals of the measures were calculated, and a P value (alpha = 0.05) was calculated for comparisons. Effect sizes (Cohen's D) where calculated to relate the size of the difference to the variation between participants. Cohen's d was determined by calculating the mean difference between the knees and dividing the result by the pooled standard deviation. The general guidelines for interpreting the effect size are: 0.2 equals a small effect; 0.5 equals a moderate effect; and 0.8 equals a large effect [29]. No post-hoc adjustment for multiple comparisons was used due to the exploratory nature of this study [30].

3. Results

Twenty-seven subjects with unilateral patellofemoral pain were included in the study. Seventeen were females and the median duration of symptoms was 24 months for both males and females (Table 1).

We found a significantly lower SUV_{max} (mean difference 0.5347, p = 0.04), K_1 (mean difference 0.00126 mL min^{-1} mL^{-1}, p = 0.05) and K_i (mean difference 0.00126 mL min^{-1} mL^{-1}, p = 0.02) in the superficial part of patella on the painful side compared to the pain-free side at baseline (before exercise). Effect sizes were negligible to small (0.17 for K_1 to 0.34 for SUV_{max}). Knee loading exercises induced significantly smaller increases in SUV_{mean}, SUV_{max}, K_1 and K_i in the superficial part of patella on the painful side compared to the pain-free side. The mean difference between the knees regarding exercise induced increases were 0.2932 for SUV_{mean} (p = 0.0028), 0.5493 for SUV_{max} (p = 0.0016), 0.00395 mL min^{-1} mL^{-1} for K_1 (p = 0.005), and 0.003903 mL min^{-1} mL^{-1} for K_i (p = 0.004). The exercise induced decrease of extraction fraction was significantly larger on the painful side when compared to the pain-free side (mean difference −0.0128, p = 0.04). Effect sizes for change values ranged from small (−0.39 for extraction fraction) to medium (0.63 for SUV_{max}). Table 2 outlines the results of the baseline measures and Table 3 the results of the change values after acute knee loading. Fig. 3 illustrates an example of lower tracer uptake in the patella and higher uptake in trochlea in the painful knee compared to the pain-free knee at rest and after knee loading exercises. Graphs showing the SUV values and kinetic parameters before and after the knee loading

Table 2
Comparison of uptake values in the deep and superficial part of patella and the medial and lateral part of trochlea between pain free and painful knees at baseline in 27 patients with PFP.

Bone region	Pain-free knees N = 27 Mean (SE)	Painful knees N = 27 Mean (SE)	Difference Mean (95%CI)	Effect size	P
Patella profound					
SUV	0.5748 (0.0608)	0.5441 (0.0608)	0.0307 (−0.0568 to 0.1182)	0.07	0.4775
SUV_{max}	1.7626 (0.2460)	2.0234 (0.2460)	−0.2609 (−0.6655 to 0.1437)	−0.15	0.1966
K_1 (mL/min/ml)	0.0071 (0.00103)	0.0067 (0.0010)	0.0004 (−0.00101 to 0.0018)	0.06	0.5695
K_2 (min^{-1})	0.0174 (0.0055)	0.0199 (0.0055)	−0.0025 (−0.012 to 0.0069)	−0.09	0.5846
K_3 (min^{-1})	0.6423 (0.0579)	0.6587 (0.0579)	−0.0165 (−0.0481 to 0.0152)	−0.05	0.2953
K_i (mL/min/ml)	0.0066 (0.0010)	0.0061 (0.0010)	0.0005 (−0.0008 to 0.0019)	0.09	0.4392
Extraction fraction	0.9429 (0.019)	0.9340 (0.0190)	0.0089 (−0.016 to 0.0338)	0.09	0.4679
Patella superficial					
SUV	0.7357 (0.0606)	0.6793 (0.0606)	0.0564 (−0.0066 to 0.1195)	0.13	0.0771
SUV_{max}	2.1887 (0.2644)	1.654 (0.2644)	0.5347 (0.0232 to 1.0463)	0.34	0.0412
K_1 (mL/min/ml)	0.0102 (0.0011)	0.0089 (0.0011)	0.0013 (0.0000 to 0.0025)	0.17	0.0455
K_2 (min^{-1})	0.0220 (0.0055)	0.0214 (0.0055)	0.0006 (−0.004 to 0.005)	0.02	0.7814
K_3 (min^{-1})	0.6406 (0.0565)	0.6333 (0.0565)	0.0073 (−0.0303 to 0.0449)	0.02	0.6929
K_i (mL/min/ml)	0.0092 (0.0008)	0.0079 (0.0008)	0.0012 (0.0002 to 0.0022)	0.20	0.0173
Extraction fraction	0.9445 (0.0189)	0.9303 (0.0189)	0.0142 (−0.0094 to 0.0378)	0.14	0.2265
Trochlea lateral					
SUV	0.5402 (0.0455)	0.5233 (0.0455)	0.0169 (−0.0599 to 0.0937)	0.06	0.6547
SUV_{max}	1.2969 (0.1596)	1.3782 (0.1596)	−0.0813 (−0.4389 to 0.2763)	−0.07	0.6442
K_1 (mL/min/ml)	0.008 (0.0011)	0.0075 (0.0011)	0.0005 (−0.0009 to 0.0019)	0.09	0.4485
K_2 (min^{-1})	0.0320 (0.0149)	0.0299 (0.0149)	0.0021 (−0.0045 to 0.0087)	0.03	0.5184
K_3 (min^{-1})	0.5942 (0.0624)	0.5908 (0.0624)	0.0035 (−0.0319 to 0.0388)	0.01	0.8423
K_i (mL/min/ml)	0.0065 (0.0007)	0.0063 (0.0007)	0.0002 (−0.0006 to 0.0010)	0.05	0.5882
Extraction fraction	0.9022 (0.0308)	0.9040 (0.0308)	−0.0018 (−0.0287 to 0.0251)	−0.01	0.8893
Trochlea medial					
SUV	0.583 (0.0457)	0.5995 (0.0457)	−0.0165 (−0.0963 to 0.0632)	−0.06	0.6738
SUV_{max}	1.3205 (0.1645)	1.513 (0.1645)	−0.1925 (−0.5921 to 0.2072)	−0.18	0.3314
K_1 (mL/min/ml)	0.0093 (0.0013)	0.0091 (0.0013)	0.0002 (−0.0013 to 0.0016)	0.02	0.82
K_2 (min^{-1})	0.0332 (0.0134)	0.0342 (0.0134)	−0.001 (−0.0083 to 0.0063)	−0.01	0.7784
K_3 (min^{-1})	0.5718 (0.0627)	0.5614 (0.0627)	0.0104 (−0.0342 to 0.0549)	0.03	0.6363
K_i (mL/min/ml)	0.0071 (0.0007)	0.0073 (0.0007)	−0.0001 (−0.0011 to 0.0009)	−0.03	0.8148
Extraction fraction	0.8735 (0.0354)	0.8785 (0.0354)	−0.005 (−0.027 to 0.0169)	−0.03	0.6413

SUV = mean standardized uptake value; SUV_{max} = maximal standardized uptake value; K_1 = bone perfusion; k_2 = tissue clearance; k_3 = mineralization; K_i = tracer plasma clearance.

Table 3
Changes after three sets of 10 repetitions of one-legged decline squat in the pain-free and painful knees together with knee differences in the response to exercise.

Change in	Pain-free knees N = 27 Mean (SE)	Painful knees N = 27 Mean (SE)	Difference Mean (95%CI)	Effect size	P
Patella profound					
SUV	1.3532 (0.2814)	1.2125 (0.2814)	0.1407 (−0.0366 to 0.318)	0.30	0.1182
SUV_{max}	3.1419 (0.6012)	3.2251 (0.6012)	−0.0832 (−0.7509 to 0.5845)	−0.05	0.8048
K_1 (mL/min/ml)	0.0252 (0.00666)	0.0234 (0.00666)	0.0019 (−0.0001 to 0.0038)	0.36	0.0617
K_2 (min^{-1})	0.0107 (0.0096)	0.0021 (0.0096)	0.0086 (−0.0002 to 0.0174)	0.37	0.0552
K_3 (min^{-1})	0.0039 (0.0679)	−0.0134 (0.0679)	0.0172 (−0.0107 to 0.0452)	0.24	0.2236
K_i (mL/min/ml)	0.0204 (0.0042)	0.0186 (0.0042)	0.0018 (−0.0002 to 0.0038)	0.35	0.0738
Extraction fraction	−0.0343 (0.0365)	−0.0232 (0.0365)	−0.0111 (−0.0341 to 0.0119)	−0.19	0.3387
Patella superficial					
SUV	1.3578 (0.2503)	1.0646 (0.2503)	0.2932 (0.1043 to 0.4821)	0.59	0.0028
SUV_{max}	3.5309 (0.5726)	2.9816 (0.5726)	0.5493 (0.2144 to 0.8841)	0.63	0.0016
K_1 (mL/min/ml)	0.0293 (0.0078)	0.0254 (0.0078)	0.0040 (0.0013 to 0.0067)	0.56	0.0046
K_2 (min^{-1})	0.0079 (0.0078)	0.0084 (0.0078)	−0.0005 (−0.0046 to 0.0037)	−0.04	0.8183
K_3 (min^{-1})	−0.0224 (0.0643)	−0.0171 (0.0643)	−0.0053 (−0.029 to 0.0185)	−0.08	0.6616
K_i (mL/min/ml)	0.0217 (0.0038)	0.0177 (0.0038)	0.0039 (0.0013 to 0.0065)	0.57	0.0041
Extraction fraction	−0.0524 (0.0377)	−0.0396 (0.0377)	−0.0128 (−0.0252 to −0.0004)	−0.39	0.0435
Trochlea lateral					
SUV	0.7101 (0.1428)	0.8038 (0.1428)	−0.0938 (−0.1781 to −0.0095)	−0.43	0.0297
SUV_{max}	1.8702 (0.3778)	2.0978 (0.3778)	−0.2275 (−0.6518 to 0.1967)	−0.21	0.2889
K_1 (mL/min/ml)	0.0161 (0.0035)	0.01714 (0.0035)	−0.00103 (−0.0022 to 0.0001)	−0.35	0.0745
K_2 (min^{-1})	−0.0086 (0.0153)	−0.0054 (0.0153)	−0.0032 (−0.0095 to 0.0032)	−0.19	0.3238
K_3 (min^{-1})	−0.0604 (0.0695)	−0.0574 (0.0695)	−0.003 (−0.0446 to 0.0386)	−0.03	0.8854
K_i (mL/min/ml)	0.013 (0.0023)	0.01398 (0.0023)	−0.00099 (−0.002 to −0.0000)	−0.40	0.0431
Extraction fraction	−0.0264 (0.0344)	−0.0275 (0.0344)	0.0011 (−0.0216 to 0.0238)	0.02	0.9248
Trochlea medial					
SUV	0.6786 (0.1188)	0.71 (0.1188)	−0.0314 (−0.1074 to 0.0447)	−0.16	0.414
SUV_{max}	1.706 (0.3031)	1.7684 (0.3031)	−0.0623 (−0.3335 to 0.2089)	−0.09	0.6486
K_1 (mL/min/ml)	0.0169 (0.0035)	0.01921 (0.0035)	−0.00236 (−0.0038 to −0.0009)	−0.62	0.0019
K_2 (min^{-1})	−0.0003 (0.0139)	0.002 (0.0139)	−0.0023 (−0.0075 to 0.0029)	−0.17	0.3775
K_3 (min^{-1})	−0.0819 (0.0629)	−0.1001 (0.0629)	0.0181 (−0.0069 to 0.0432)	0.28	0.1529
K_i (mL/min/ml)	0.0129 (0.0024)	0.01424 (0.0024)	−0.0014 (−0.0023 to −0.0005)	−0.57	0.0039
Extraction fraction	−0.0317 (0.0376)	−0.0527 (0.0376)	0.021 (0.0049 to 0.0371)	0.50	0.0111

SUV = mean standardized uptake value; SUV_{max} = maximal standardized uptake value; K_1 = bone perfusion; k_2 = tissue clearance; k_3 = mineralization; K_i = tracer plasma clearance.

exercises are provided in Fig. 4, and magnitude of the exercise induced changes are provided in supplementary files, Fig. S1.

The results for the normalized values at baseline resembled the results for the raw values, although SUV_{max} and K_1 were not statistically significant (p = 0.06 and 0.1, respectively). For the profound part of patella and the lateral and medial part of trochlea, uptake parameters did not differ between painful and pain-free knees at baseline. For the change values of the normalized data, SUV_{mean}, SUV_{max}, K_1, K_i, and extraction fraction was significantly lower in the painful side compared to the pain-free side in the profound part of patella, but not in the superficial part. Tables for the normalized values are provided in the supplementary files, Tables S1–2.

In trochlea, we found no significant difference in raw (Table 2) or normalized (Table S2) values between the painful and the pain-free knees at baseline for any uptake parameters. We found significantly greater increases after the knee loading exercises in the painful than the pain free knees for SUV_{mean} (mean difference −0.0938, p = 0.03) and K_i (mean difference −0.00099, p = 0.04) in the lateral part of trochlea (effect sizes −0.43 and −0.40, respectively). For the medial part of trochlea, the painful knees also had greater increases of K_1 (mean difference −0.00236, p = 0.002) and K_i (mean difference −0.00138, p = 0.004), and a greater decrease in extraction fraction (mean difference 0.021, p = 0.01). The tendency was the same for the normalized values with a few discrepancies (supplemental files, Table S2).

4. Discussion

This study compared both resting subchondral bone turnover and the post exercise hemodynamic response in patients with unilateral patellofemoral pain and revealed distinctive differences between the painful and pain-free knees. Our data demonstrate that individuals with patellofemoral pain have reduced tracer uptake in the patella but increased uptake in the subchondral region of the trochlea on the painful side compared to the pain-free side following acute knee loading. Moreover, we found reduced tracer uptake, blood flow, and bone turnover in the superficial part of the patella in the painful knees at rest. These findings could suggest that the metabolism and perfusion of the patella bone is decreased and may undergo hypoxic conditions mainly after loading exercise. In contrast, increases in flow and tracer uptake was present in the trochlea, mainly after acute loading. The results offer new insights into the blood flow and bone turnover of the patellofemoral joint, thereby contributing to our understanding of the disorder's complex etiology.

The lower bone turnover and blood flow in the painful patella indicate a decreased bone turnover in comparison to the pain-free knees at rest. Notably, these differences were confined to the superficial part of the patella. In the trochlea, no difference was observed between the painful and pain-free knees for any tracer uptake parameter at rest. The baseline results contrast with previous studies, which reported increased tracer uptake in the compartments of the patellofemoral joint [21,31]. This may be attributable to methodological disparities. The previous cross-sectional studies had inadequate statistical power to compare knees with pain to those without pain, and they were limited in their ability to conduct within-individual comparisons. Also, no standardization of participant activities prior to examination was reported in these studies [21,31]. In the present study, we minimized the effect of prior knee loading activities by asking the participants to refrain from exercising, knee-loading labor, stair climbing etc. prior to assessments and we refunded expenses for transportation to the hospital to promote compliance with unloading the knees. It has been shown, that knee loading induces an acute response in bone physiology as quantified by [^{18}F]NaF tracer uptake [20].

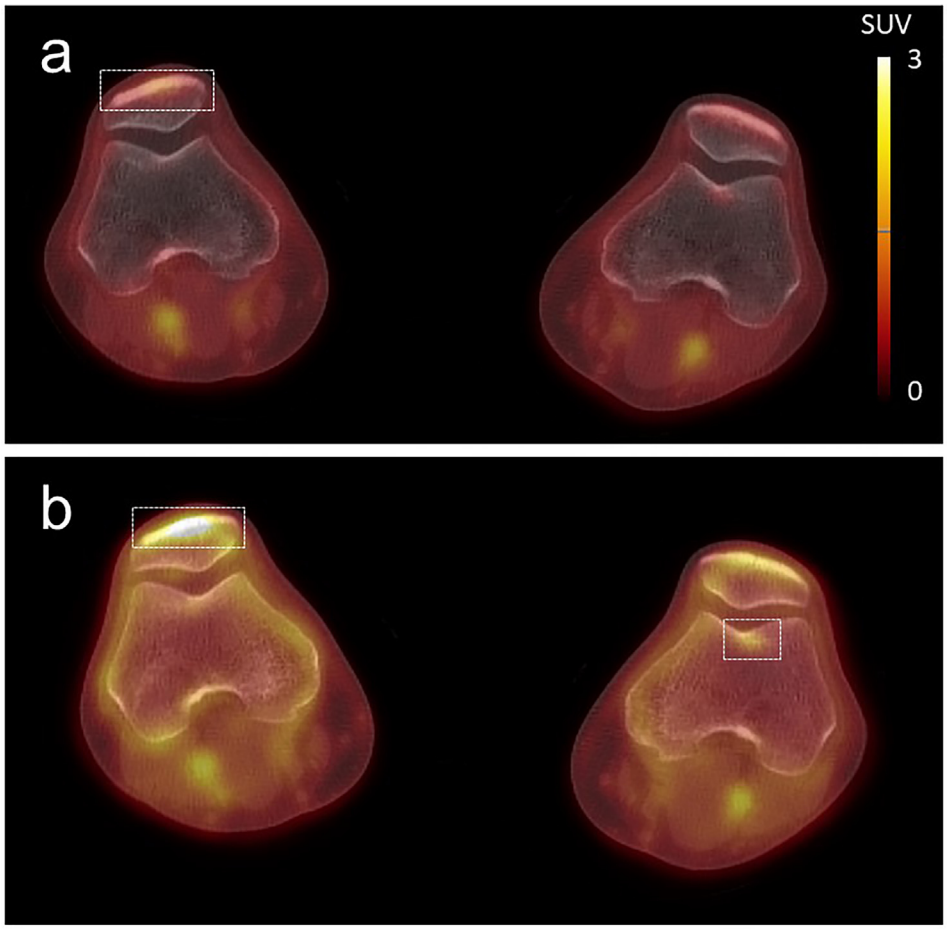

Fig. 3. Representative axial Na[^{18}F]F PET images of the femur and patella at rest (a) and after knee loading (b). The images display higher SUV values in the patella of the pain-free knee (right knee, left side of image) compared to the painful knee (right side of image), as well as a localized area of increased SUV in the trochlea of the painful knee after exercise. The scale bar denotes SUV values, and the dashed squares indicate focal areas of increased SUV.

In the current study, the exercise-induced increases in mean and maximal uptake values (SUV_{mean} and SUV_{max}), the rate of tracer uptake (K_i) and blood flow (K_1) were attenuated in the painful knees compared to the pain-free knees in the superficial part of the patella. This observation supports the findings by Näslund et al., which demonstrated a reduction of blood flow in the patella in PFP patients compared with healthy controls when passively flexing the knee to 90° [32]. Also, a recent study by Ophey et al. found impaired patella hemodynamics in patients with PFP compared to healthy controls when descending stairs [33]. Collectively, these findings suggest a potential involvement of a lower blood perfusion in the pathogenesis of PFP [32]. Decreased perfusion, hypoxia, and intra-osseous hypertension are recognized as a pathophysiological mechanism in OA [34–36]. However, it remains uncertain whether the extent of altered blood flow observed in the patella in this study is sufficient to induce ischemic or hypoxic conditions in the subchondral bone. At present, no specific threshold for blood perfusion that would lead to pain has been established. Also, it remains unknown whether the altered blood flow seen in the patella and trochlea of the present study is causal or a consequence of long-term pain. Accordingly, care must be taken when interpreting the results.

In trochlea, changes in several uptake parameters values were higher in the painful knees compared with pain-free knees, which support previous studies (12, 22). Specifically, the changes in rate of tracer uptake (K_i) were higher in both lateral and medial part of trochlea with moderate effect sizes (0.4 and 0.57, respectively), presumably driven by increases in flow (K_1). In the lateral part of trochlea, the change in mean SUV was higher in the painful knee, while for the medial part, there were significantly higher changes for K_1, K_i, and a lower extraction fraction.

A study on rats has demonstrated an increase in [^{18}F]NaF uptake following acute loading, showing a correlation with the magnitude of force exerted upon the bone [37]. Watkins et al. documented analogous findings in knee osteoarthritic patients subjected to a single-legged knee extension exercise until fatigue [18]. Substantial alterations in [^{18}F]NaF uptake were discerned in bones exhibiting osteophytes, bone marrow lesions, and concomitant cartilage loss, with the most pronounced increases occurring in the patella. In the present study, we extend previous PET studies investigating PFP by introducing a knee-loading exercise regime (one--legged squatting) that allowed us to compare joint tissue response in the painful with the pain-free knees. Our data indicate that while part of the patella bone shows decreased bone turnover and perfusion, the subchondral bone of the trochlea exhibits contrasting behavior, possibly indicating a reparative process associated with knee pain. Previous research suggests that pain may stem from nociceptive substance-P fibers within abnormal erosion channels of subchondral bone in the degenerative and osteoarthritic PFJ joint [11]. This could explain why higher patella water content has been observed in PFP which may lead to increased intraosseous pressure and pain during mechanical loading [38,39].

Our study has several limitations. One is the cross-sectional design that inherently limits interpretation of causality. However, the inclusion of an internal control in the study design mitigates the interparticipant variability often encountered in cross-sectional studies. It is important to acknowledge that individuals with PFP often experience bilateral pain [7, 40], and there is speculation that unilateral pain may precede bilateral pain [41,42]. Thus, a pain-free knee may not be considered a truly healthy control. Future research might consider including a healthy control group.

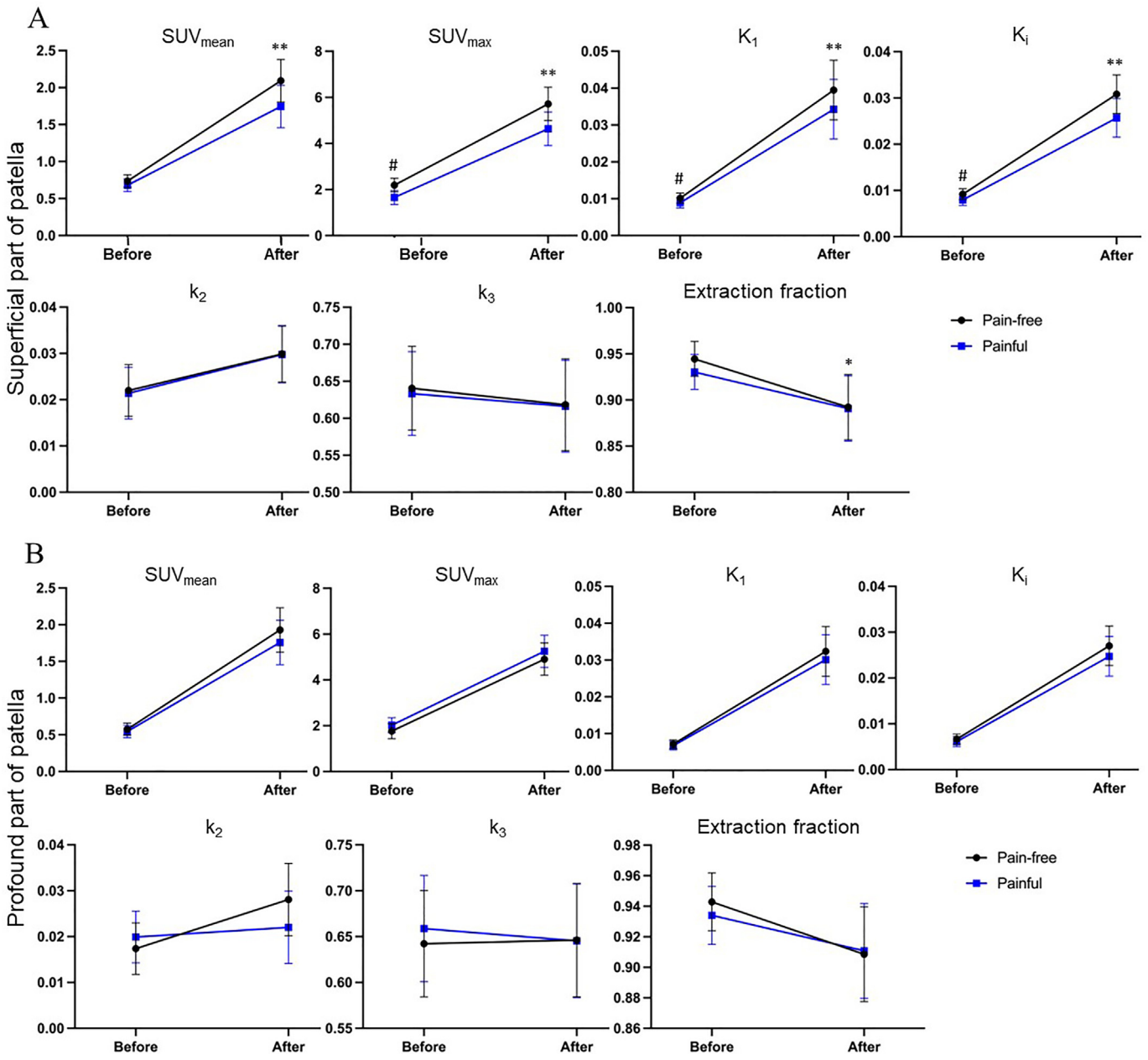

Fig. 4. The mean and maximal Standardized Uptake Value (SUV_{mean} and SUV_{max}) and kinetic uptake parameters K_1, k_2, k_3, K_i, and extraction fraction in the profound part of patella (A), the superficial part of patella (B), the lateral part of trochlea (C) and the medial part of trochlea (D) before and after a bout of 10 times three one-legged squats on a decline board.
# indicates a statistically significant difference ($p < 0.05$) at baseline between painful and pain-free knees; * indicates a statistically significant difference ($p < 0.05$) in change between painful and pain-free knees; ** indicates a statistically significant difference ($p < 0.01$) in change between painful and pain-free knees.

Errors in the estimation of dynamic [^{18}F]NaF uptake parameters can arise from inaccuracies in the arterial input function, a measure of the activity delivered to the region of interest through the arterial system. Here, we used an IDIF using measures of activity in the popliteal artery and calibrating the input function with measures of venous blood at 30, 40, 50, and 60 min after injection. The repeatability and accuracy of the input function has been presented elsewhere [20]. By calibrating the IDIF to the actual tracer concentration in the blood, we improve the accuracy of IDIF quantification. Further limitations to the quantification of tracer uptake also include the assumption that the tracer is bound irreversibly to bone and approximating the rate k_4 to 0. This assumption is generally believed to be sensible due to the small value and poor precision of k_4 [43].

One significant limitation is the potential for participants to have consciously or unconsciously reduced the load on their painful knee during daily activities and/or during the loading protocol, which could result in a reduced uptake of the tracer in PET scans. We made extensive efforts to ensure that participants performed the single-leg squats equally on both legs by using a goniometer and providing verbal instructions to reach the desired knee angle. Additionally, the increased bone perfusion and tracer extraction observed in the trochlea of the painful knees supports the notion that unloading was less likely. While participants were encouraged to avoid strenuous physical activities, their activity prior to assessment was not monitored. The sample size was set pragmatically and based on the inclusion in the main study. The study may therefore be underpowered to detect clinically meaningful differences. The study is,

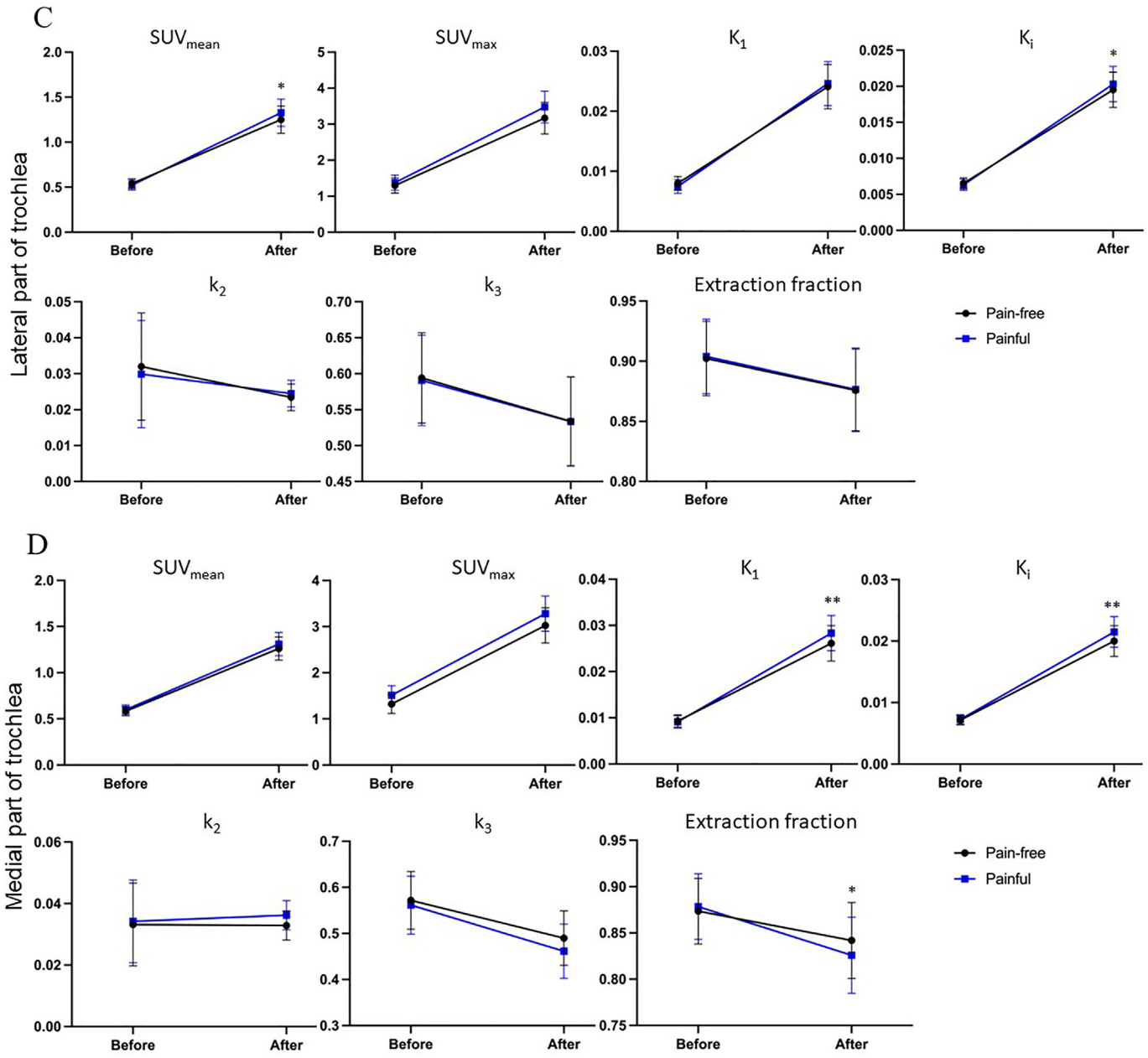

Fig. 4. (*continued*).

however, the largest to date investigating bone turnover in patients with patellofemoral pain. Finally, this study was explorative in nature, and hence we did not adjust for multiplicity. The results are indicative rather than conclusive and should be confirmed in future studies.

5. Conclusion

We found that bone turnover (SUV_{max} and K_i) and blood flow (K_1) were lower in the patella on the painful side compared to the pain-free side at rest. After knee loading exercises, the acute increases in uptake (SUV_{mean}, SUV_{max}, and K_i) and blood flow (K_1) were substantially reduced in the superficial part of the patella on the painful side compared to the pain-free side. On the contrary, the acute change in tracer uptake was higher in the lateral part of trochlea (SUV_{mean} and K_i) and the medial part of the trochlea (K_i, K_1) and the decrease in extraction fraction was larger in the painful compared to the pain-free knees. Collectively, our data suggests a differential bone turnover and blood flow dynamics in the patellofemoral joint that could be associated with symptoms and etiology in PFP.

Author contributions

All authors contributed equally to the study and made substantial contributions to the conception or design of the study, drafting the paper, and reviewing it critically and all approved the final paper and agree to be accountable for all aspects of the work.

Data collection and analysis were performed by RH, MH, BH, RS, IR, ML and CC. Data analysis methods including developing applications and creating scripts in Matlab was done by BH. LR had the medical responsibility for the PET/CT scans and ensured that we did not overlook other pathology. CB assessed for eligibility. MH, RS and SPM were responsible for the statistical analysis. The first draft of the manuscript was written by RH.

Declaration of competing interests

The authors declare that they have no known competing financial interests or personal relationships that could have appeared to influence the work reported in this paper.

Acknowledgements

This research was funded by the internal research funds of Bispebjerg and Frederiksberg Hospital. We would like to express our gratitude to the radiographers Martin Reinholt Jensen and Asger Raza Müller for their exceptional work in performing the PET/CT scans for all study participants.

Appendix A. Supplementary data

Supplementary data to this article can be found online at https://doi.org/10.1016/j.ocarto.2025.100583.

References

[1] M.S. Rathleff, C.R. Rathleff, J.L. Olesen, S. Rasmussen, E.M. Roos, Is knee pain during adolescence a self-limiting condition? Prognosis of patellofemoral pain and other types of knee pain, Am. J. Sports Med. 44 (5) (May 2016) 1165–1171, https://doi.org/10.1177/0363546515622456.

[2] N.E. Lankhorst, M. van Middelkoop, K.M. Crossley, et al., Factors that predict a poor outcome 5-8 years after the diagnosis of patellofemoral pain: a multicentre observational analysis, Br. J. Sports Med. 50 (14) (Jul 2016) 881–886, https://doi.org/10.1136/bjsports-2015-094664.

[3] M.S. Rathleff, L. Winiarski, K. Krommes, et al., Pain, sports participation, and physical function in adolescents with patellofemoral pain and osgood-schlatter disease: a matched cross-sectional study, J. Orthop. Sports Phys. Ther. 50 (3) (Mar 2020) 149–157, https://doi.org/10.2519/jospt.2020.8770.

[4] B.E. Smith, J. Selfe, D. Thacker, et al., Incidence and prevalence of patellofemoral pain: a systematic review and meta-analysis, PLoS One 13 (1) (2018) e0190892, https://doi.org/10.1371/journal.pone.0190892.

[5] K.M. Crossley, M.J. Callaghan, R. van Linschoten, Patellofemoral pain, Br. J. Sports Med. 50 (4) (Feb 2016) 247–250, https://doi.org/10.1136/bjsports-2015-h3939rep.

[6] R.A. Dutton, M.J. Khadavi, M. Fredericson, Patellofemoral pain, Phys. Med. Rehabil. Clin 27 (1) (Feb 2016) 31–52, https://doi.org/10.1016/j.pmr.2015.08.002.

[7] K.M. Crossley, J.J. Stefanik, J. Selfe, et al., 2016 Patellofemoral pain consensus statement from the 4th International Patellofemoral Pain Research Retreat, Manchester. Part 1: terminology, definitions, clinical examination, natural history, patellofemoral osteoarthritis and patient-reported outcome measures, Br. J. Sports Med. 50 (14) (Jul 2016) 839–843, https://doi.org/10.1136/bjsports-2016-096384.

[8] R.A. van der Heijden, N.E. Lankhorst, R. van Linschoten, S.M. Bierma-Zeinstra, M. van Middelkoop, Exercise for treating patellofemoral pain syndrome, Cochrane Database Syst. Rev. 1 (Jan 20 2015) CD010387, https://doi.org/10.1002/14651858.CD010387.pub2.

[9] C.A. Thorstensson, M.L. Andersson, H. Jonsson, T. Saxne, I.F. Petersson, Natural course of knee osteoarthritis in middle-aged subjects with knee pain: 12-year follow-up using clinical and radiographic criteria, Ann. Rheum. Dis. 68 (12) (Dec 2009) 1890–1893, https://doi.org/10.1136/ard.2008.095158.

[10] K.M. Crossley, Is patellofemoral osteoarthritis a common sequela of patellofemoral pain? Br. J. Sports Med. 48 (6) (Mar 2014) 409–410, https://doi.org/10.1136/bjsports-2014-093445.

[11] E.M. Wojtys, D.N. Beaman, R.A. Glover, D. Janda, Innervation of the human knee joint by substance-P fibers, Arthroscopy 6 (4) (1990) 254–263, https://doi.org/10.1016/0749-8063(90)90054-h.

[12] M.B. Goldring, S.R. Goldring, Articular cartilage and subchondral bone in the pathogenesis of osteoarthritis, Ann. N. Y. Acad. Sci. 1192 (Mar 2010) 230–237, https://doi.org/10.1111/j.1749-6632.2009.05240.x.

[13] D.B. Burr, M.A. Gallant, Bone remodelling in osteoarthritis, Nat. Rev. Rheumatol. 8 (11) (Nov 2012) 665–673, https://doi.org/10.1038/nrrheum.2012.130.

[14] S. Donell, Subchondral bone remodelling in osteoarthritis, EFORT Open Rev 4 (6) (Jun 2019) 221–229, https://doi.org/10.1302/2058-5241.4.180102.

[15] W.N. Newberry, D.K. Zukosky, R.C. Haut, Subfracture insult to a knee joint causes alterations in the bone and in the functional stiffness of overlying cartilage, J. Orthop. Res. 15 (3) (May 1997) 450–455, https://doi.org/10.1002/jor.1100150319.

[16] J.P. Dyke, M. Synan, P. Ezell, D. Ballon, J. Racine, R.K. Aaron, Characterization of bone perfusion by dynamic contrast-enhanced magnetic resonance imaging and positron emission tomography in the Dunkin-Hartley Guinea pig model of advanced osteoarthritis, J. Orthop. Res. 33 (3) (Mar 2015) 366–372, https://doi.org/10.1002/jor.22768.

[17] J. Benske, M. Schunke, B. Tillmann, Subchondral bone formation in arthrosis. Polychrome labeling studies in mice, Acta Orthop. Scand. 59 (5) (Oct 1988) 536–541, https://doi.org/10.3109/17453678809148779.

[18] L.E. Watkins, B. Haddock, J.W. MacKay, et al., [(18)F]Sodium fluoride PET-MRI detects increased metabolic bone response to whole-joint loading stress in osteoarthritic knees, Osteoarthr. Cartil. 30 (11) (Nov 2022) 1515–1525, https://doi.org/10.1016/j.joca.2022.08.004.

[19] L. Aaltonen, N. Koivuviita, M. Seppanen, et al., Correlation between (18)F-Sodium Fluoride positron emission tomography and bone histomorphometry in dialysis patients, Bone 134 (May 2020) 115267, https://doi.org/10.1016/j.bone.2020.115267.

[20] B. Haddock, A.P. Fan, S.D. Uhlrich, et al., Assessment of acute bone loading in humans using [(18)F]NaF PET/MRI, Eur. J. Nucl. Med. Mol. Imag. 46 (12) (Nov 2019) 2452–2463, https://doi.org/10.1007/s00259-019-04424-2.

[21] C.E. Draper, M. Fredericson, G.E. Gold, et al., Patients with patellofemoral pain exhibit elevated bone metabolic activity at the patellofemoral joint, J. Orthop. Res. 30 (2) (Feb 2012) 209–213, https://doi.org/10.1002/jor.21523.

[22] D. Savic, V. Pedoia, Y. Seo, et al., Imaging bone-cartilage interactions in osteoarthritis using [(18)F]-NaF PET-MRI, Mol. Imaging 15 (Jan 1 2016) 1–12, https://doi.org/10.1177/1536012116683597.

[23] D. Hayashi, F.W. Roemer, A. Guermazi, Imaging of osteoarthritis by conventional radiography, MR imaging, PET-computed tomography, and PET-MR imaging, Pet. Clin. 14 (1) (Jan 2019) 17–29, https://doi.org/10.1016/j.cpet.2018.08.004.

[24] R. Hansen, C. Brushoj, M.S. Rathleff, S.P. Magnusson, M. Henriksen, Quadriceps or hip exercises for patellofemoral pain? A randomised controlled equivalence trial, Br. J. Sports Med. 57 (20) (Oct 2023) 1287–1294, https://doi.org/10.1136/bjsports-2022-106197.

[25] P.C. Charlton, A.L. Bryant, J.L. Kemp, R.A. Clark, K.M. Crossley, N.J. Collins, Single-leg squat performance is impaired 1 to 2 Years after hip arthroscopy, Pharm. Manag. PM R 8 (4) (Apr 2016) 321–330, https://doi.org/10.1016/j.pmrj.2015.07.004.

[26] B. Haddock, A.P. Fan, N.R. Jorgensen, C. Suetta, G.E. Gold, F. Kogan, Kinetic [18F]-Fluoride of the knee in normal volunteers, Clin. Nucl. Med. 44 (5) (May 2019) 377–385, https://doi.org/10.1097/RLU.0000000000002533.

[27] R.A. Hawkins, Y. Choi, S.C. Huang, et al., Evaluation of the skeletal kinetics of fluorine-18-fluoride ion with PET, J. Nucl. Med. 33 (5) (May 1992) 633–642.

[28] R.F. Muzic Jr., S. Cornelius, COMKAT: compartment model kinetic analysis tool, J. Nucl. Med. 42 (4) (Apr 2001) 636–645.

[29] J. Cohen, Statistical Power Analysis for the Behavioral Sciences, Routledge Academic, 1988.

[30] R. Bender, S. Lange, Adjusting for multiple testing–when and how? J. Clin. Epidemiol. 54 (4) (Apr 2001) 343–349, https://doi.org/10.1016/s0895-4356(00)00314-0.

[31] J.E. Naslund, S. Odenbring, U.B. Naslund, T. Lundeberg, Diffusely increased bone scintigraphic uptake in patellofemoral pain syndrome, Br. J. Sports Med. 39 (3) (Mar 2005) 162–165, https://doi.org/10.1136/bjsm.2004.012336.

[32] J. Naslund, M. Walden, L.G. Lindberg, Decreased pulsatile blood flow in the patella in patellofemoral pain syndrome, Am. J. Sports Med. 35 (10) (Oct 2007) 1668–1673, https://doi.org/10.1177/0363546507303115.

[33] M.J. Ophey, A. Westerweel, M. van Oort, R. van den Berg, G. Kerkhoffs, I.J.R. Tak, Impaired hemodynamics of the patella in patients with patellofemoral pain: a case-control study, J Exp Orthop 11 (1) (Jan 2024) e12009, https://doi.org/10.1002/jeo2.12009.

[34] C.C. Arnoldi, Vascular aspects of degenerative joint disorders. A synthesis, Acta Orthop. Scand. Suppl. 261 (Aug 1994) 1–82.

[35] T. Kiaer, J. Gronlund, K.H. Sorensen, Subchondral pO2, pCO2, pressure, pH, and lactate in human osteoarthritis of the hip, Clin. Orthop. Relat. Res. 229 (Apr 1988) 149–155.

[36] T. Kiaer, N.W. Pedersen, K.D. Kristensen, H. Starklint, Intra-osseous pressure and oxygen tension in avascular necrosis and osteoarthritis of the hip, J Bone Joint Surg Br 72 (6) (Nov 1990) 1023–1030, https://doi.org/10.1302/0301-620X.72B6.2246284.

[37] R.E. Tomlinson, M.J. Silva, K.I. Shoghi, Quantification of skeletal blood flow and fluoride metabolism in rats using PET in a pre-clinical stress fracture model, Mol. Imag. Biol. 14 (3) (Jun 2012) 348–354, https://doi.org/10.1007/s11307-011-0505-3.

[38] K.Y. Ho, H.H. Hu, P.M. Colletti, C.M. Powers, Recreational runners with patellofemoral pain exhibit elevated patella water content, Magn. Reson. Imaging 32 (7) (Sep 2014) 965–968, https://doi.org/10.1016/j.mri.2014.04.018.

[39] O. Miltner, C.H. Siebert, U. Schneider, F.U. Niethard, J. Graf, Patellar hypertension syndrome in adolescence: a three-year follow up, Arch. Orthop. Trauma Surg. 123 (9) (Nov 2003) 455–459, https://doi.org/10.1007/s00402-003-0564-2.

[40] N. Steinberg, S. Tenenbaum, G. Waddington, et al., Unilateral and bilateral patellofemoral pain in young female dancers: associated factors, J. Sports Sci. 38 (7) (Apr 2020) 719–730, https://doi.org/10.1080/02640414.2020.1727822.

[41] M.C. Waiteman, R.V. Briani, H.S. Lopes, et al., People with patellofemoral pain have bilateral deficits in physical performance regardless of pain laterality, J. Athl. Train. (Mar 13 2024), https://doi.org/10.4085/1062-6050-0649.23.

[42] S.A. Boudreau, A.C. Royo, M. Matthews, et al., Distinct patterns of variation in the distribution of knee pain, Sci. Rep. 8 (1) (Nov 8 2018) 16522, https://doi.org/10.1038/s41598-018-34950-2.

[43] M. Siddique, M.L. Frost, G.M. Blake, et al., The precision and sensitivity of (18)F-fluoride PET for measuring regional bone metabolism: a comparison of quantification methods, J. Nucl. Med. 52 (11) (Nov 2011) 1748–1755, https://doi.org/10.2967/jnumed.111.093195.